MolecularMedicine

Effects of Erythropoietin in Murine-Induced Pluripotent Cell-Derived Panneural Progenitor Cells

Nils Offen,[1] Johannes Flemming,[1] Hares Kamawal,[1] Ruhel Ahmad,[2†] Wanja Wolber,[1] Christian Geis,[3,4] Holm Zaehres,[5] Hans R Schöler,[5] Hannelore Ehrenreich,[6] Albrecht M Müller,[2] and Anna-Leena Sirén[1]*

[1]Department of Neurosurgery, [2]Center for Experimental Molecular Medicine (ZEMM), and [3]Department of Neurology, University of Würzburg, Würzburg, Germany; [4]Department of Neurology and Center for Sepsis Control and Care (CSCC), Jena University Hospital, Jena, Germany; [5]Department of Cell and Developmental Biology, Max-Planck Institute for Molecular Biomedicine, Münster, Germany; [6]Clinical Neuroscience, Max Planck Institute of Experimental Medicine, Göttingen, Germany; *present address: Lund Stem Cell Center, Lund University, Lund, Sweden; †present address: Department of Neurosciences, University of California, San Diego, La Jolla, California, United States of America

Induced cell fate changes by reprogramming of somatic cells offers an efficient strategy to generate autologous pluripotent stem (iPS) cells from any adult cell type. The potential of iPS cells to differentiate into various cell types is well established, however the efficiency to produce functional neurons from iPS cells remains modest. Here, we generated panneural progenitor cells (pNPCs) from mouse iPS cells and investigated the effect of the neurotrophic growth factor erythropoietin (EPO) on their survival, proliferation and neurodifferentiation. Under neural differentiation conditions, iPS-derived pNPCs gave rise to microtubule-associated protein-2 positive neuronlike cells (34% to 43%) and platelet-derived growth factor receptor positive oligodendrocytelike cells (21% to 25%) while less than 1% of the cells expressed the astrocytic marker glial fibrillary acidic protein. Neuronlike cells generated action potentials and developed active presynaptic terminals. The pNPCs expressed EPO receptor (EPOR) mRNA and displayed functional EPOR signaling. In proliferating cultures, EPO (0.1–3 U/mL) slightly improved pNPC survival but reduced cell proliferation and neurosphere formation in a concentration-dependent manner. In differentiating cultures EPO facilitated neurodifferentiation as assessed by the increased number of β-III-tubulin positive neurons. Our results show that EPO inhibits iPS pNPC self-renewal and promotes neurogenesis.

Online address: http://www.molmed.org
doi: 10.2119/molmed.2013.00136

INTRODUCTION

Induced pluripotent (iPS) cells are generated by reprogramming of somatic cells by induced expression of the four transcription factors *Oct4*, *Sox2*, *Klf4* and *c-Myc* (1–3). Similar to embryonic stem cells (ESC), iPS cells are able to differentiate into all of the different cell types that comprise the organs of an adult body including neuronal subpopulations (1–6). However, individual iPS cells are heterogeneous in respect to gene expression and epigenetic patterns (7–10). Some iPS cell lines have a differentiation bias toward their cell type of origin, which seems to be linked to somatic memory mechanism, a cell-type specific epigenetic memory they retain following reprogramming (7,8,11,12). A requirement for the use of iPS cell-derived neurons for pharmacological or therapeutic applications is an efficient and stabile neurogenesis (13). Recent studies have indicated a role for the activin/nodal, BMP, Notch, Shh or Fgf pathways (6,14) as well as several miRNAs (15) to exit the pluripotent state and to initiate differentiation.

Hypoxia promotes self-renewal and proliferation of tissue-specific stem cells and ESCs (16). In human iPS cells, hypoxia promotes reprogramming and enhances iPS cell production (17) and neuronal differentiation (18). Hypoxia also is a potent inducer of gene expression of the hematopoietic growth factor erythropoietin (EPO) (19). EPO and its receptor (EPOR) are best known for their role in regulating erythroid proliferation and differentiation (19) but EPO and EPOR also are expressed in the nervous system (20) where they exert potent cytoprotective and trophic activities (20–23). A substantial amount of effort has been devoted to characterize the mechanism of the neuroregenerative actions of EPO (24,25). For example, inhibition of apoptosis and inflammation seem to mediate EPO-induced neuroprotection after acute

Address correspondence to *Anna-Leena Sirén, Experimental Neurosurgery, University of Würzburg, Josef-Schneider Str. 11, 97080 Würzburg, Germany. Phone: +49-931-201-24 579; Fax: +49-931-201-24 140; E-mail: siren.a@nch.uni-wuerzburg.de.*
Submitted October 21, 2013; Accepted for publication November 6, 2013; Epub (www.molmed.org) ahead of print November 7, 2013.

The Feinstein Institute for Medical Research North Shore LIJ

brain injuries (24,25) while the trophic and myelination promoting effects of EPO may be important for its ability to counteract chronic neurodegeneration and neuroinflammation (26–29). Direct effects on neural stem cells also may play a role in the neurorestorative actions of EPO in rodent models of ischemic and traumatic brain injury (30–33). In these *in vivo* models, EPO improves injury-induced neurogenesis (31–33) and stimulates oligodendrogliosis (33). Accordingly, deletion of EPOR in the nervous system reduces the size of the neural stem cell pool and impairs injury-induced adult neurogenesis (30,34). Hypoxic preconditioning of neural stem cells induces EPO and improves neuronal differentiation (35) but it is not known whether EPO can stimulate neurogenesis from pluripotent stem cells. In this study, we examined whether EPO and EPOR play a role in the generation of neuronal cells from iPS cells. For this purpose we first characterized neurogenesis of iPS cells (1), and studied the effects of EPO on proliferation and neurodifferentiation of the iPS cell-derived neural progenitor cells.

MATERIAL AND METHODS

iPS/ES Cell Maintenance

For all experiments, iPS cells reprogrammed from murine neural stem cells by ectopic *Oct4*, *Klf4*, *c-Myc* and *Sox2* expression, expressing *lacZ* from the rosa26 locus and carrying a Oct4-GFP transgene (1) were used. The mouse ESC wtB1 cell line carrying a β-actin-GFP transgene (36) was used as a positive control for pluripotent gene expression (Figure 1C). Cells were cultured on inactivated murine embryonic fibroblasts (MEF) in 60-mm plates (BD Biosciences, Heidelberg, Germany) in DMEM medium supplemented with 15% FCS, 1% nonessential amino acids, 1% penicillin/streptomycin, 1 mmol/L sodium pyruvate, 2 mmol/L L-glutamate, 10 mmol/L 4-(2-hydroxyethyl)-1-piperazineethanesulfonic acid (HEPES) (all from PAA Laboratories GmbH, Hamburg, Germany), 0.1 mmol/L β-mercaptoethanol (Sigma-Aldrich, Taufkirchen, Germany) and leukemia inhibitory factor at 37°C/5% CO_2 and passaged every 2–3 d. Medium was changed every second day. For passaging, cells were washed once with PBS and detached from the culture plates by trypsin/EDTA (PAA Laboratories GmbH) treatment for 5 min at 37°C. The reaction was stopped after 5 min with DMEM medium supplemented with 10% FCS and cells were collected, washed and replated onto fresh feeders.

Neural Differentiation of iPSC Cultures

iPS cells and ESCs were differentiated into panneural progenitor cells (pNPCs) using a monolayer differentiation protocol (37) with the following modifications: iPS cells and ESCs were passaged and the cells were plated onto 100 mm plates (Greiner Bio-One, Frickenhausen, Germany) coated with 0.1% gelatin from bovine skin in PBS (Sigma-Aldrich) and incubated at 37°C to separate iPS/ES cells and MEFs. After 45 min, iPS or ES cells were collected from the gelatin-coated plates, washed, counted and replated on gelatin-coated 60 mm plates (BD Biosciences) in GMEM medium (Life Technologies GmbH, Darmstadt, Germany) supplemented with 10% FCS, 1% penicillin/streptomycin, 2 mmol/L L-glutamate, 10 mmol/L HEPES (all from PAA Laboratories GmbH), 0.1 mmol/L β-mercaptoethanol (Sigma-Aldrich) and leukemia inhibitory factor with a density of 400,000 cells/plate for iPS cells and 200,000 cells/plate for ESCs. After 24 h, medium was replaced with N2B27 medium (37) and cells were differentiated for 5 d at 37°C/5% CO_2. N2B27 medium was changed every second day.

Expansion of pNPCs

pNPCs were washed once with PBS and detached from the culture plates with trypsin/EDTA (PAA Laboratories GmbH) for 5 min at 37°C , washed and plated in 25-cm^2 suspension culture flasks (Greiner Bio-One) with a density of 1,000,000–1,500,000 cells per flask and cultured in 7 mL pNPC medium composed of DMEM/F12 medium supplemented with 2 mmol/L L-glutamate, 15 mmol/L HEPES, 0.22% sodium bicarbonate, 2% B27 without vitamin A (all from Life Technologies GmbH), 1% penicillin/streptomycin (PAA Laboratories GmbH), 0.6 g glucose (Sigma-Aldrich), 20 ng/mL hEGF and 20 ng/mL bFGF2 (both from Peprotech, Hamburg, Germany). pNPCs were cultured at 37°C under 5% CO_2/95% air and 90% humidity for 5 to 6 d. Medium was replaced every third day.

pNPC-generated spheres were passaged on d 5 or 6 according to the following protocol: pNPC-spheres were first incubated in AccuMax (PAA Laboratories GmbH) for 5 min at 37°C and mechanically triturated into single cells with a fire-polished Pasteur pipette. pNPCs were replated in 7 mL pNPC medium density of 1,000,000–1,500,000 cells per flask.

Analysis of Oct4-GFP Fluorescence

GFP fluorescence was analyzed with an Olympus IX70 fluorescence microscope (Olympus, Münster, Germany) and images were taken using the Analysis software (Soft Imaging System GmbH, Münster, Germany). In addition, the loss of GFP fluorescence during differentiation was analyzed by flow cytometry. Cells at d 0 and 5 of differentiation were detached from the culture plates as described, collected, washed, resuspended in PBS (Sigma-Aldrich) and analyzed using a BD FACSCanto and FACSDiva software (BD Biosciences). FACS data was analyzed using the software Weasel.

Differentiation of pNPCs

Secondary pNPC-spheres were dissociated into single cells and plated on poly-D-lysine (PDL; Sigma-Aldrich) coated glass coverslips (Paul Marienfeld GmbH & Co KG, Lauda-Königshofen, Germany) in 24-well cell culture plates (Greiner Bio-One) at a density of 25,000 cells/well in B27 medium consisting of neurobasal medium supplemented with 2% B27 (both from Life Technologies

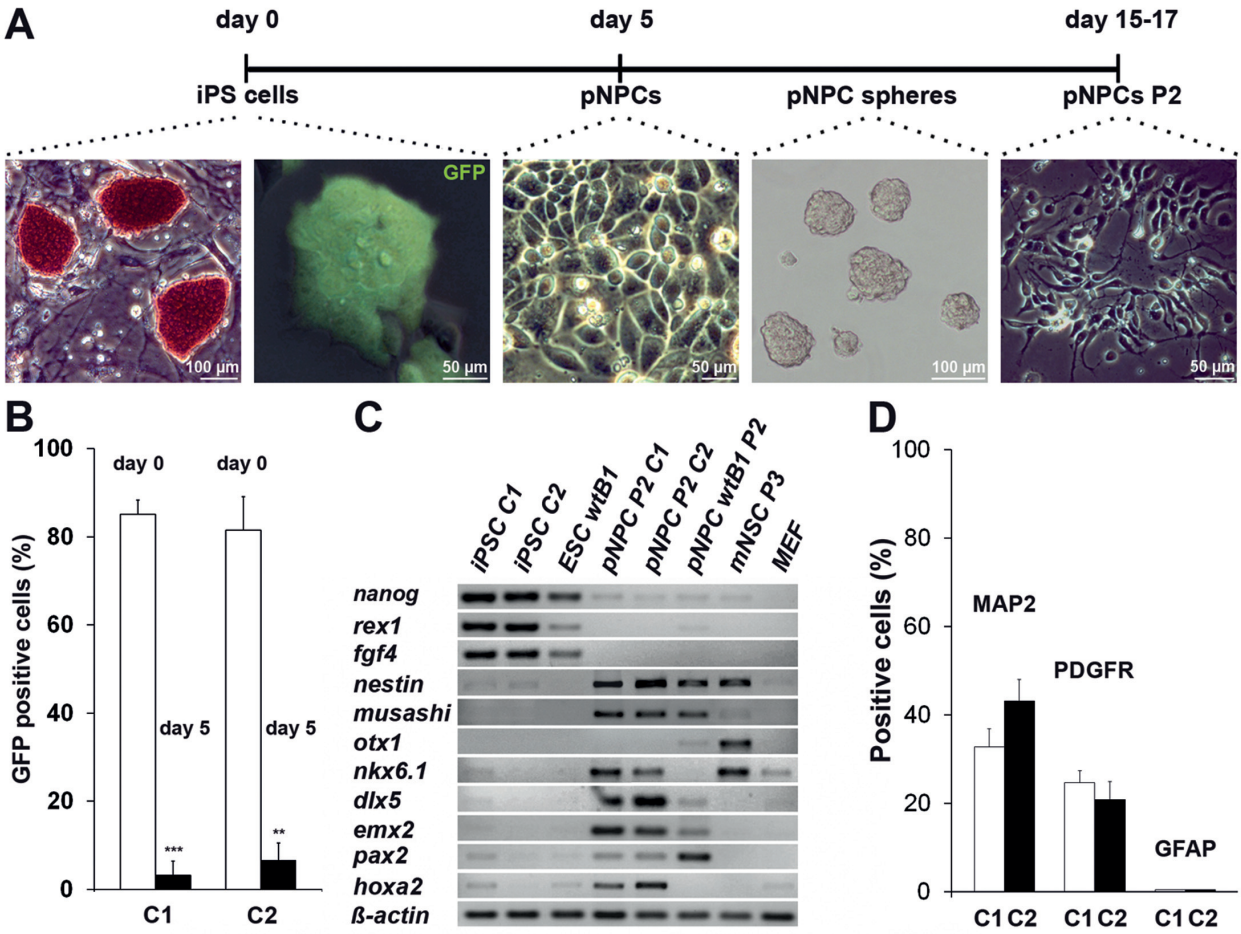

Figure 1. Characterization of *in vitro* neurogenesis of iPS cells and neural differentiation of iPS pNPCs. (A) Time scale diagram for neural differentiation of iPS cells and pNPC expansion as neurospheres. Left panel shows typical alkaline phosphatase positive iPS cell colonies (red). The rest of the panels depict overlays of phase contrast images and the GFP signal of Oct-4-driven GFP. iPS cells were positive for GFP; pNPCs, neurospheres and expanded pNPCs were negative for GFP. (B) FACS quantification of the Oct-4-GFP positive cells (P1) at d 0 and d 5 of differentiation for clonal line 1 (C1) and 2 (C2). Data are represented as mean ± SD, n = 3. (C) Expression analysis of different pluripotency and neural genes by RT-PCR in iPS cells and pNPCs. Mouse embryonic stem cell line (ESC wtB1), wtB1-derived pNPCs, neural stem cells (mNSC) and mouse embryonic fibroblasts (MEF) were used as controls. (D) Percentage of cells from C1 and C2 expressing markers for neurons (MAP-2), oligodendrocytes (PDGFR) and astrocytes (GFAP) at d 10 of differentiation. Data is represented as mean ± SD, n = 3. (E) Representative images of marker expression during pNPC differentiation. At d 0 of differentiation cells expressed the neural stem cell marker nestin and the neuronal progenitor marker Pax6. After 10 d in culture pNPCs expressed the neuronal markers MAP-2 and TAU, the astrocytic marker GFAP and the oligodendrocytic marker PDGFR. Staining for the oligodendrocyte marker O4 became visible after 14 d of differentiation. After 22 d, cells expressed the presynaptic marker synapsin, the postsynaptic marker homer1 and myelin basic protein, a marker for mature oligodendrocytes. (F) Immunochemical labeling of active synapses. Fluorescent picture showing staining for synapsin (green), and synaptotagmin I (red) and the mask for analyzing the frequency of colocalized dots (yellow, arrowhead). Graph shows the quantification of the mean percentage of double stained dots. Data represent mean ± SD, n = 3. (G) Electrophysiological characterization of pNPCs at d 13/14. I/V curves of VC-stimulation in pNPC C1 neuronlike cells before and after treatment with ttx (tetrodotoxin, sodium channel blocker) or TEA (tetraethylamonium, potassium channel blocker). Stimulation potential (mV) is plotted against the maximum measured inward or outward current (current was normalized to cell size (pA/pF), data represent mean ± SD; n = 6, $*p < 0.05$, $**p < 0.01$ (paired *t* test for normal and Wilcoxon test for not normal distributed samples). A representative trace of membrane potential responding to step depolarization by current injection (depolarizations: black lines; hyperpolarizations: gray lines) and a representative trace of whole cell currents in voltage clamp mode responding to step depolarization by current injection. Current injections (–50 pA, +10 pA) into pNPC-derived neurons in current clamp (CC)-mode. Stimulation via stepwise increase of membrane potential (–80 mV to +55 mV, step size 15 mV) in VC-mode. Scale bars (A): first and fourth subpanels from left, 100 µm; second, third and fifth subpanels from left, 50 µm; (E): top subpanels and second through fourth bottom subpanels, 25 µm; first and fifth bottom subpanels, 10 µm.

Continued on the next page

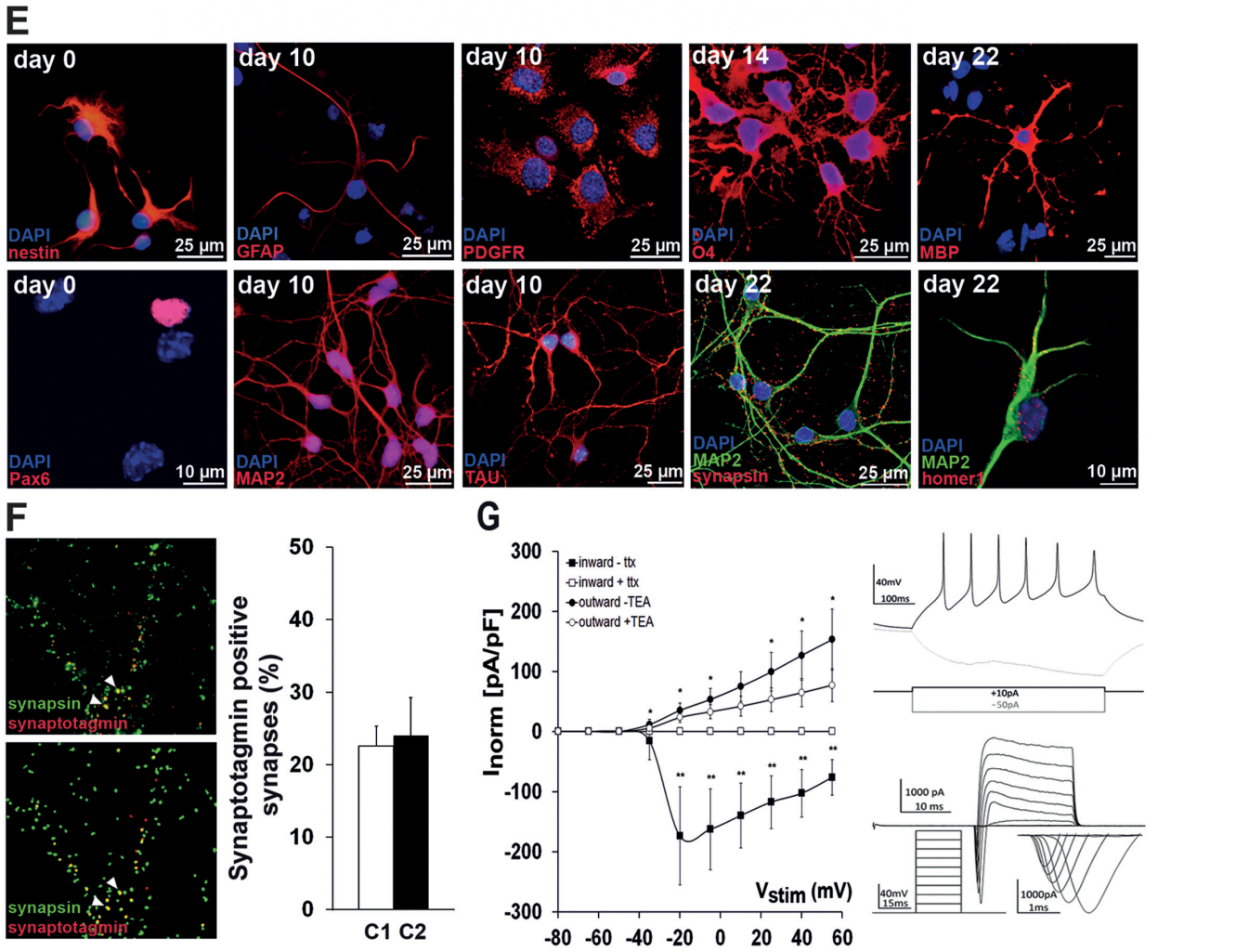

Figure 1. ***Continued.***

GmbH), 1% penicillin/streptomycin and 2 mmol/L L-glutamine (both from PAA Laboratories GmbH). pNPCs were cultured at 37°C under 5% CO_2/95% air and 90% humidity and medium was replaced every fourth day.

RT PCR

Total RNA was isolated using TRIzol (Life Technologies GmbH) according to the manufacturer's instructions. 1 µg of total RNA was treated with 1 U DNAseI (Fermentas, St. Leon-Rot, Germany) for 40 min at 37°C to remove remaining DNA. mRNA was transcribed into cDNA with the Maxima Reverse transcriptase (Fermentas) at 50°C for 60 min. cDNA fragments from the genes of interest were amplified by standard PCR using gene-specific primers (Supplementary Table S1). Mouse β-actin primers were used as internal standard.

Immunocytochemistry

pNPCs were fixed for 20 min in 4% PFA (Sigma-Aldrich) after 0, 10, 14 or 22 d in differentiation, permeabilized and blocked in 0.2% Triton X-100 (Roche, Penzberg, Germany) with 10% normal horse serum (NHS) in phosphate buffered saline (PBS) (Dianova, Hamburg, Germany) for 30 min. Cells were then incubated with primary antibodies (Supplementary Table S2) against neural cell markers in 1% NHS at 4°C overnight, followed by incubation with a secondary antibody (Supplementary Table S2) in 1% NHS for 1 h. Cells were mounted in Mowiol with 4′,6-diamidino-2-phenylindole (DAPI) for nuclear counter staining. Cells were photographed with a Leica LSM TCS SP5 confocal microscope (Leica, Wetzlar, Germany). Images were processed using the ImageJ software (MBF ImageJ for Microscopy) (38) and CorelDRAW Graphics Suite X5.

Cell Counting

pNPCs differentiated for 10 d were fixed and stained for microtubule-associated protein 2 (MAP-2), glial fibrillary acidic protein (GFAP) or platelet-derived growth factor receptor α

(PDGFRα) as described above. For each marker, photos from three coverslips (five randomly chosen fields/coverslip) were taken using an Axiophot2 fluorescence microscope (Zeiss, Jena, Germany) with a SPOT Insight camera (Visitron Systems, Puchheim, Germany). From each image taken the number of living and dead (DAPI) as well as MAP-2, GFAP or PDGFR positive cells were counted. The experiment was replicated twice.

Synaptic Vesicle Recycling

pNPCs differentiated for 22 d, were incubated with a rabbit anti-synaptotagmin I antibody (1:00, Synaptic Systems, Göttingen, Germany) against the luminal domain of the protein in high potassium Krebs-Ringer-HEPES buffer (KRH) (55 mmol/L KCl, 85 mmol/L NaCl, 10 mmol/L HEPES, pH 7.4, 10 mmol/L glucose, 2.6 mmol/L $CaCl_2$ and 1.3 mmol/L $MgCl_2$) for 1 min at 37°C. The antibody solution was removed and cells were washed thrice in KHR buffer (5 mmol/L KCl, 140 mmol/L NaCl, 10 mmol/L HEPES, pH 7.4, 10 mmol/L glucose, 2.6 mmol/L $CaCl_2$ and 1.3 mmol/L $MgCl_2$) for 5 min. Cells were fixed and incubated with a mouse-anti-synapsin I antibody (1:1,000; Synaptic Systems) followed by an incubation with a goat anti-mouse-DL488 and goat anti-rabbit-Cy3 antibody (1:1,000, both from Dianova, Hamburg, Germany) as described above. Photographic images from three coverslips (three randomly chosen fields/coverslip) were taken using an Axiophot2 fluorescence microscope with a SPOT Insight camera. Pictures were processed in ImageJ (38) using the following protocol: images were smoothed using a gaussian filter with $\sigma = 2$, Laplace filtered and thresholded to isolate small maxima in fluorescence intensity corresponding to synaptic buttons. To increase the signal-to-noise ratio a particle filter with a threshold of 16 pixels was applied. The total number of synapsin I positive buttons and the number of buttons colocalizing with synaptotagmin I staining were counted. The experiment was replicated twice.

Whole Cell Patch-Clamp Analysis

Cells were transferred into a recording chamber and continuously superfused with extracellular solution containing 125 mmol/L NaCl, 25 mmol/L $NaHCO_3$, 25 mmol/L glucose, 2.5 mmol/L KCl, 1.25 mmol/L NaH_2PO_4, 2 mmol/L $CaCl_2$, 2 mmol/L $MgCl_2$ purged by 95% CO_2/5% O_2. The ion channel antagonists tetraethylammonium chloride (TEA) or tetrodotoxin (ttx) (both from Sigma-Aldrich) were added to the extracellular solution with a concentration of 30 mmol/L and 1 μmol/L, respectively. All experiments were performed at room temperature using an EPC 10 double patch clamp amplifier and pulse software (HEKA, Lambrecht, Germany). Electrodes were pulled from thick-walled borosilicate glass (Warner Instruments, Hamden, CT, USA) and filled with intracellular solution (120 mmol/L K-gluconate, 32 mmol/L KCl, 10 mmol/L HEPES, 4 mmol/L NaCl, 0.5 mmol/L EGTA, 4 mmol/L MgATP, 0.4 mmol/L Na_2-GTP, pH 7.2, 290-300 $mOsml^{-1}$) and had a resistance between 4 and 6 MΩ. Cells were held in whole-cell configuration at –70 mV and were discarded if the series resistance was higher than 25 MΩ at the beginning of the measurements.

EPOR Activity Assay

Activation of the EPOR-associated signaling was investigated by Western blot analysis of the phosphorylation of ERK 1/2. Secondary pNPC-spheres were dissociated into single cells as described above and seeded into 25-cm^2 suspension culture flasks with a density of 1,500,000 cells. After 24 h, 1 U/mL human recombinant EPO (epoetin beta, NeoRecormon, Roche, Welwyn Garden City, UK) or PBS was added to the suspension culture and total cell protein was extracted 5 min after treatment using PhosphoSafe (Merck, Darmstadt, Germany) according to the manufacturer's instructions. Protein concentration was measured with the BCA Protein Assay (Thermo Fisher Scientific, Schwerte, Germany) and stored afterward at –80°C. Five volumes of protein solution were mixed with 1 volume of Laemmli buffer (250 mmol/L Tris HCl, pH 8.3, 8% SDS, 40% glycerol, 20% 2-mercaptoethanol, 0.04% pyronin Y) and boiled for 5 min at 95°C. Ten to fifteen μg protein was run on 15% polyacrylamide gels (Roth, Karlruhe, Germany) for 2 h at 150 V and transferred to a nitrocellulose membrane for 1 h at 400 mA using a miniVE electrophoresis and electro transfer unit (Amersham Bioscience/GE Healthcare, Munich, Germany). After blocking with 5% milk powder in Tween20-Tris-buffered saline (TTBS), at room temperature for 1 h, the membranes were incubated with primary antibodies for mouse anti-pMAPK (1:2,000, Sigma-Aldrich) or rabbit anti-MAPK (1:5,000, Sigma-Aldrich). Immunoreactive bands were visualized using a secondary anti-mouse (1:5,000) or anti-rabbit (1:15,000) antibody coupled to horseradish peroxidase (both from Sigma-Aldrich) by enhanced chemiluminescence (ECL Prime Western blotting detection kit, Amersham Bioscience/GE Healthcare). Densitometric analysis of protein bands was performed using the ImageJ software.

Cell Survival Assay

For the pNPC survival assay, secondary spheres were dissociated into single cells and plated at a density of 50,000 cells on PDL coated glass coverslips in 24-well cell culture plates. pNPCs were cultured in B27 medium with 0.1, 1 or 10 U/mL EPO or PBS. After 24 h or 48 h MTT cell survival assay was performed according to the following protocol: pNPCs were incubated in B27 medium supplemented with 30 mmol/L thiazolyl-blue-tetrazolium-bromide (MTT; Sigma-Aldrich) for 2 h at 37°C/5% CO_2. Cells were washes with PBS and treated for 5 min with cell lysis buffer (50% *N*,*N*-dimethylformamide, 20% sodium dodecylsulfat, pH 4.7). The absorption of the

formazan product that is produced by metabolization of the MTT reagent was measured at 570 nm. Cell vitality of the EPO treated cells was calculated from the absorption as follows:

Cell vitality [%] =
Mean Abs_{570nm} EPO treatment/
Mean Abs Abs_{570nm} control treatment
× 100.

Control was set as 100%. Four independent experiments in six replicates of every treatment group were performed for each clone.

pNPC Dilution Assay

Secondary pNPC-spheres were dissociated into single cells and seeded with a density of 1, 10, 25, 50, 100, 250, 500, 750, 1000, 1500 or 2500 cells per well into 96-well suspension culture plates (Greiner Bio-One) containing 200 µL of pNPC medium. Cells were treated immediately either with 0.3 or 1 U/mL EPO or placebo and cultured for 7 d without changing the medium. At d 7, all spheres/well were photographed using an Olympus IX70 inverse microscope and the Analysis software and counted. Sphere diameter was measured using ImageJ (38). Analysis was performed blinded. Four independent experiments were performed for each clone. For each experiment, three replicates of every treatment group were analyzed.

pNPC Proliferation Assay

Single pNPCs derived from secondary spheres were labeled with 0.2 µmol/L carboxyfluorescein-succinimidyl-ester (CFSE) (Sigma-Aldrich) in PBS (1,000,000 cells/mL) for 10 min at 37°C, mixture of ice-cold PBS and pNPC medium without hEGF and bFGF2 was added and cells were incubated for 5 min on ice followed by three washing steps in PBS. Immediately after washing an aliquot of CFSE-labeled and unlabeled cells were analyzed using a BD FACSCanto and FACSDiva software.

Labeled cells were seeded into 25-cm^2 suspension culture flasks with a density of 1,000,000 cells/flask and grown in pNPC medium supplemented with 1 U/mL EPO or placebo. After 48 h, newly formed pNPC-spheres were dissociated into single cells and analyzed by flow cytometry. FACS data was evaluated using Weasel software. For each clone, four independent experiment were performed.

In a separate set of experiments, CFSE-labeled cells were incubated in 5 mL pNPC medium without growth factors containing either DMSO, 10 µmol/L LY294002 or 10 µmol/L U0126. After 20 min, placebo or 1 U/mL EPO was added and cells were incubated for an additional hour. Afterward, cells were washed twice in PBS and seeded into 25-cm^2 suspension culture flasks in 5 mL pNPC medium and incubated at 37°C under 5% CO_2/ 95% air and 90% humidity. After 48 h, CFSE fluorescence was analyzed by flow cytometry as described above. For each clone, three to four independent experiments were performed.

Cell Cycle Analysis

pNPCs were derived from secondary spheres as described above. One million cells in 5 mL pNPC medium were incubated in the presence of 5 µg/mL aphidicolin (SERVA Electrophoresis GmbH, Heidelberg, Germany) for 14 h. After 14 h, cells were washed twice in PBS and incubated in 5 mL pNPC medium supplemented with 1 U/mL EPO or placebo for 10 and 24 h. Afterward, cells were washed twice in PBS and fixed in 3% PFA for 15 min. After fixation cells were washed once in PBS and stained in 500 µL PBS containing 50 µg/mL propidium iodide (PI, Sigma-Aldrich), 0.1 mg/mL RNAseA (Fermentas) and 0.05% Triton X-100 for 40 min at 37°C. PI labeled cells were analyzed using a FACSCanto and FACSDiva software. FACS data was evaluated using Weasel software. For each clone, three to four independent experiments were performed.

Neuronal Differentiation Assay

Secondary spheres were dissociated into single cells and plated on PDL coated glass coverslips in 24-well cell culture plates with a density of 12,500 cells/coverslip and grown in B27 medium with 3 U/mL EPO or placebo. After 2, 4 or 6 d, cells were fixed and stained with a mouse-anti-β-III-tubulin primary (1:500, Sigma-Aldrich) and an anti-mouse-Cy3 (1:1000, Dianova) secondary antibody, and counterstained with DAPI. Pictures from two coverslips (eight randomly chosen fields/coverslip) were taken using an Axiophot2 fluorescence microscope with a SPOT Insight camera. The number of living (DAPI) and β-III-tubulin (TuJ1)-positive cells was counted. In addition, the length of each process of TuJ1-positive cells was measured using the NeuronJ plugin for the ImageJ software (21). Cells with processes shorter than the cell soma's diameter were excluded from further analysis. Measurements and data analysis was performed blinded.

Statistical Analysis

Data are expressed as mean ± SD for indicated number of repetitions (n). Data were tested for normal distribution using a graphical approach (quantile-quantile Plot) and the Shapiro–Wilk test. Group differences with normal distribution were analyzed by Student *t* test and the Wilcoxon test was used for not normally distributed datasets. Data plotting and statistical analysis were done using Microsoft Excel and R (39). Differences were considered significant at $p < 0.05$.

All supplementary materials are available online at www.molmed.org.

RESULTS

Neurogenesis of iPS Cells

To assess the potential of iPS cells for *in vitro* neurogenesis, we first induced their differentiation into pNPCs by culturing the cells for 5 d followed by pNPC expansion as neurospheres for additional 10 to 12 d (Figure 1A). During neural differentiation the iPS cells lost the expression of an *Oct-4*-driven GFP- transgene within 5 d (Figures 1A,1B). At this stage, the pNPCs were negative for the pluripotency genes

Nanog, *Rex1* and *Fgf4* (Figure 1C) and started to express neural stem cell markers *nestin* and *musashi* (see Figure 1C). As expected, pNPCs but not iPS cells expressed genes involved in forebrain (*Emx2*, *Dlx5*) or midbrain/hindbrain development (*Nkx6.1*, *Dlx2* and *Hoxa2*) (40–42).

Neural Differentiation and Maturation of iPS pNPCs

When the cells were cultured under neuronal differentiation conditions for 10 d pNPCs became positive for neuronal and glial markers (Figure 1D,1E). Counting of frequencies of neural cell types after 10 d of differentiation (see Figure 1D) revealed that 33% (clonal line C1) and 43% (clonal line C2) of all cells expressed the neuron-specific protein, microtubule-associated-protein 2 (MAP2), whereas 25% (C1) and 21% (C2) expressed the oligodendrocyte marker platelet-derived growth factor receptor (PDGFR). Less than 1% of all cells were positive for the astrocyte specific protein, glial fibrillary acidic protein (GFAP) (see Figure 1D). Figure 1E shows representative images of cells at various stages of differentiation. Immediately after plating iPS pNPCs were positive for the neural precursor marker nestin. Some of them also expressed the neuronal progenitor marker Pax6 (see Figure 1E). In 10 d old cultures, the expression of the neuronal markers MAP2 and TAU as well as the oligodendrocyte marker PDGFR were prominent and the astrocyte marker GFAP was detectable in few cells. Staining for the oligodendrocyte marker O4 (see Figure 1E) and the presynaptic marker synapsin became visible after 14 d of differentiation. After 22 d in culture, synapsin expression was pronounced and cells expressed the postsynaptic marker homer1 (see Figure 1E). Expression of myelin basic protein (MBP), a marker for mature oligodendrocytes became also detectable after 22 d in culture (see Figure 1E). At this stage of *in vitro* maturation, roughly one fourth (23% to 24%) of the neuronlike cells showed the presence of active presynaptic terminals after induction of presynaptic vesicle fusion by a brief exposure to 55 mmol/L KCl (Figure 1F).

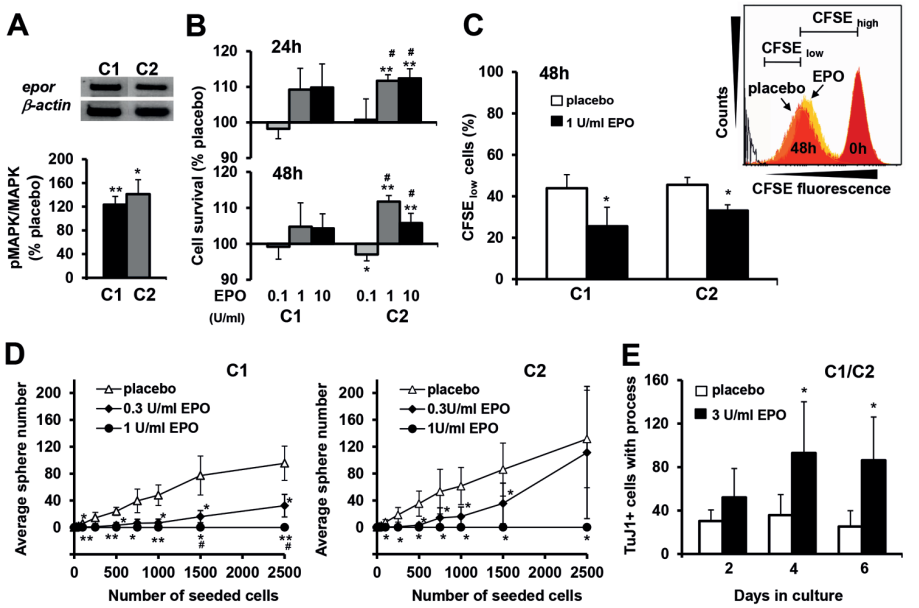

Figure 2. Effect of EPO on iPS pNPCs. (A) pNPCs express EPOR mRNA and functional EPOR: EPO treatment leads to an increase in ERK1,2 (MAPK) phosphorylation (n = 6, C1; n = 4, C2). (B) Effect of EPO treatment on cell survival after 24 h and 48 h (n = 4 in each group). (C) Effect of EPO on pNPC proliferation (n = 4 in each group). The percentage of fast proliferating cells (cells gated with low CFSE signal in inset) is decreased in both clonal lines after EPO treatment. (D) Effect of EPO on sphere formation under different seeding concentration (n = 4 in each group). (E) The number of TuJ1-positive neurons in cultures treated with placebo or EPO (1 U/mL) (n = 4 in each group). The average number of living cells per field was 19 ± 7 (placebo) and 29 ± 13 (EPO) for d 2, 19 ± 7 (placebo) and 22 ± 11 (EPO) for d 4 and 17 ± 8 (placebo) and 16 ± 5 (EPO) for d 6, respectively. Data represent mean ± SD for the indicated number of samples, $^{*}p < 0.05$, $^{**}p < 0.01$ versus placebo, $^{\#}p < 0.05$ versus EPO 0.1 U/mL (B) or versus EPO 0.3 U/mL (D); *t* test for normal and Wilcoxon test for not normal distributed samples.

To further confirm that the iPS-derived neuronlike cells develop functional neuronal properties, we performed whole cell patch clamp recordings at d 13 and 14 of differentiation. The cells were stimulated in current clamp (CC) mode with depolarizing current injections (–50 pA to +130 pA, step size 20 pA) over a time period of 500 ms. In 11 out of 16 (C1) and 10 out of 20 (C2) recorded cells current injection elicited action potentials, multiple action potentials could be elicited (Figure 1G). The average resting membrane potential for the recorded cells was –44.81 ± 9.01 mV (C1) and –48.38 ± 13.38 mV (C2), respectively. In voltage clamp (VC) mode we stepwise depolarized the cells (–80 mV to +55 mV, step size 15 mV) to induce action potentials and measured the corresponding inward and outward currents. Neuronlike cells from both clonal lines showed a similar pattern of maximum inward and outward currents plotted against the voltage stimulus, however C2 showed a tendency for lower outward currents compared with clone 1 (Figure 1G and not shown). As expected, treatment of cells with the Na^+-channel inhibitor tetrodotoxin (ttx) or the K^+-channel inhibitor tetraethylammonium (TEA) completely abolished inward (Na^+) and reduced outward (K^+) currents (see Figure 1G).

Effect of EPO on iPS pNPCs

We first confirmed that pNPCs from both iPS clones express EPOR mRNA and functional EPOR by monitoring the EPO-induced activation of MAPK signaling (Figure 2A). When the cells were cultured for 24 h under different concentra-

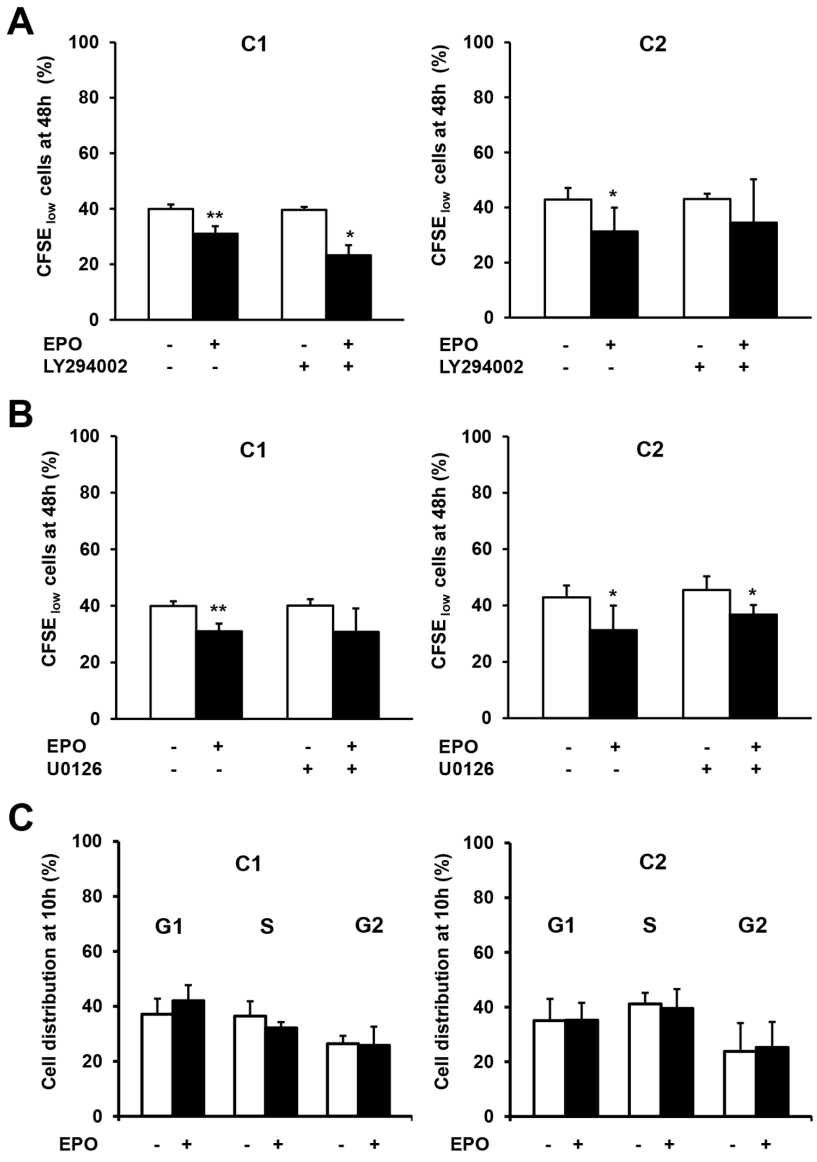

Figure 3. iPS pNPC proliferation and cell cycle analysis. The PI3K inhibitor LY294002 (A) or the MAPK-inhibitor U-0126 (B) have no consistent effect on EPO-induced reduction of pNPC proliferation (percentage of $CFSE_{low}$ cells after 48 h). (C) Cell cycle analysis of pNPC proliferation. EPO treatment did not change the percentage of cells in G1, S or G2-phase after 10 h of treatment in either clonal lines. Data in all panels represent mean ± SD, n = 3 (C1), n = 4 (C2); $*p < 0.05$, $**p < 0.01$ (paired *t* test for normal and Wilcoxon test for not normal distributed samples).

tions of EPO, cell survival in C2 was improved by EPO concentrations of 1 U/mL and 10 U/mL (Figure 2B). A tendency for a better cell survival after EPO also was observed in C1 (see Figure 2B). A similar pattern of cell survival also was seen in cells cultured for 48 h (see Figure 2B). When the effect of EPO on cell proliferation was tested by CFSE cell proliferation assay, EPO (1 U/mL) reduced cell proliferation in both cell clones (Figure 2C). Since binding of EPO to EPOR activates ERK1/2 and Akt-1 signaling in neurons (21–23), we tested whether pretreatment with inhibitors of these pathways can modify the effect of EPO on pNPC proliferation. Treatment with the PI3K-inhibitor LY294002 (10 μmol/L) or the MAPK inhibitor U0176 (10 μmol/L) failed to influence the antiproliferative effect of EPO consistently (Figures 3A–B). Cell cycle analysis of pNPCs showed no changes in cell cycle progression after EPO treatment (Figure 3C).

To analyze the effect of EPO on neurosphere formation, pNPCs were plated with different densities from 1 up to 2,500 cells/well and were allowed to form spheres for 7 d in the presence of 0.3 or 1 U/mL EPO or placebo. After 7 d, EPO suppressed sphere formation in a dose dependent manner (Figure 2D). For assessment of the effect of EPO on neuronal differentiation, pNPCs were cultured under culture conditions favoring differentiation in the presence or absence of 3 U/mL EPO. EPO treatment more than doubled the number of TuJ1-positive neurons at d 4 and 6 (Figure 2F). Together this indicates that EPO facilitated neurodifferentiation of iPS-derived pNPCs.

DISCUSSION

Efficient generation of neural cell types from pluripotent embryonic or iPS cells have been the subject of intensive research (6,14,43–46), but factors that lead to a robust formation of pNPCs from pluripotent stem cells and/or their differentiation into neural subtypes still need to be identified. In the present study we first show that the hematopoietic growth factor EPO directs iPS pNPC neurogenesis into neuronal fate by inhibiting proliferation and promoting neuronal differentiation.

We first confirmed the potential of iPS cells to generate proliferating pNPCs, which further differentiated into mature neurons and oligodendrocytes. iPS cell-derived neuronlike cells showed the ability to generate action potentials, possessed membrane characteristics similar to newly formed neurons (47,48) and were capable of forming active presynaptic terminals. In this regard our findings are in accordance with several other

studies that showed the ability of murine iPS cell lines to generate different neural subtypes, including functional neurons (6,45,49,50). The iPS cell-derived progenitors in our study produced mainly neurons and oligodendrocytes. In contrast to earlier studies showing the generation of 10% astrocytes from murine iPSCs (6,51), we detected less than 1% astrocytes. These differences might be explained by differences in the reprogramming process and the origin of the somatic cell used for iPS cell generation, as our cells might have a differentiation bias toward neurons due to their type of origin (1,5,43,52,53). Culture conditions such as the concentration of EGF and bFGF2 in culture media also may have influenced the neural cell fates (54,55).

In the second part of the study, we analyzed the potential of EPO to modulate neurogenesis in two clones of iPS pNPCs which expressed functional EPOR. We observed that EPO increased cell viability of pNPCs. This is not surprising given the fact that the antiapoptotic and cytoprotective effects of EPO have been reported in several *in vivo* and *in vitro* experimental settings (25). An alternative explanation for the increase in viable cells after EPO treatment would be a stimulation of cell proliferation. However, we found that EPO had an inhibitory effect on cell proliferation. Treatment with EPO thus seems to improve the maintenance of a homogenous and stabile neural cell type. Furthermore, the competence of pNPCs to form spheres was drastically reduced by EPO. In agreement with our findings, Shingo and colleagues described an inhibitory effect of EPO on neurosphere formation and growth from neural stem cells isolated from fetal rat brain (35). Others have reported stimulation of proliferation of adult neural stem cells in response to EPO treatment (34,56–58). These opposing results may be related to different cell culture types and to the use of higher EPO concentrations.

MAPK and PI3/AKT signaling have been shown to support neurosphere formation and/or growth in neural stem cells (59). These signaling pathways also have been shown to be activated by EPO in neurons (21–23,28,57,60). Even if iPS cell-derived pNPCs expressed EPOR mRNA and functional EPOR-associated intracellular signaling pathways, neither inhibition of MAPK nor PI3K/AKT counteracted the effect of EPO on iPS pNPC proliferation. Therefore, relevant pathways mediating the EPO-induced inhibition of cell proliferation remain to be determined.

Finally, we show that in differentiating cultures of iPS pNPCs treatment with EPO led to increased numbers of TuJ1-positive neurons. These findings agree with previous reports on EPO-induced improvements in neuronal differentiation of fetal and adult neural stem cells (35,61).

CONCLUSION

We generated panneural progenitor cells (pNPCs) from mouse iPS cells and investigated the effect of the neurotrophic growth factor erythropoietin on their survival, proliferation and neurodifferentiation. We show that EPO inhibits self-renewal and promotes neurogenesis of these cells. This novel effect of EPO may bear clinical relevance, as EPO might be used to improve the production and maintenance of a homogeneous and stabile neural stem cell population from human iPS cells.

ACKNOWLEDGMENTS

We thank Barbara Gado for expert technical assistance, and Christine Hofstetter and Daniela Zdzieblo, for help with the FACS analysis. This study was supported by the Interdisciplinary Center for Clinical Research (IZKF), University of Würzburg (TP D103).

DISCLOSURE

The authors declare that they have no competing interests as defined by *Molecular Medicine*, or other interests that might be perceived to influence the results and discussion reported in this paper.

REFERENCES

1. Kim JB, *et al*. (2008) Pluripotent stem cells induced from adult neural stem cells by reprogramming with two factors. *Nature*. 454:646–50.
2. Robinton DA, Daley GQ. (2012) The promise of induced pluripotent stem cells in research and therapy. *Nature*. 481:295–305.
3. Takahashi K, Yamanaka S. (2006) Induction of pluripotent stem cells from mouse embryonic and adult fibroblast cultures by defined factors. *Cell*. 126:663–76.
4. Hu BY, *et al*. (2010) Neural differentiation of human induced pluripotent stem cells follows developmental principles but with variable potency. *Proc. Natl. Acad. Sci. U. S. A*. 107:4335–40.
5. Lohle M, *et al*. (2012) Differentiation efficiency of induced pluripotent stem cells depends on the number of reprogramming factors. *Stem Cells*. 30:570–9.
6. Salewski RP, *et al*. (2013) The generation of definitive neural stem cells from PiggyBac transposon-induced pluripotent stem cells can be enhanced by induction of the NOTCH signaling pathway. *Stem Cells Dev*. 22:383–96.
7. Kim K, *et al*. (2010) Epigenetic memory in induced pluripotent stem cells. *Nature*. 467:285–90.
8. Lister R, *et al*. (2011) Hotspots of aberrant epigenomic reprogramming in human induced pluripotent stem cells. *Nature*. 471:68–73.
9. Bar-Nur O, Russ HA, Efrat S, Benvenisty N. (2011) Epigenetic memory and preferential lineage-specific differentiation in induced pluripotent stem cells derived from human pancreatic islet beta cells. *Cell Stem Cell*. 9:17–23.
10. Hu QR, Friedrich AM, Johnson LV, Clegg DO. (2010) Memory in induced pluripotent stem cells: reprogrammed human retinal-pigmented epithelial cells show tendency for spontaneous redifferentiation. *Stem Cells*. 28:1981–91.
11. Mikkelsen TS, *et al*. (2008) Dissecting direct reprogramming through integrative genomic analysis. *Nature*. 454:49–55,794.
12. Wernig M, *et al*. (2008) Neurons derived from reprogrammed fibroblasts functionally integrate into the fetal brain and improve symptoms of rats with Parkinson's disease. *Proc. Natl. Acad. Sci. U. S. A*. 105:5856–61.
13. Kawai H, *et al*. (2010) Tridermal tumorigenesis of induced pluripotent stem cells transplanted in ischemic brain. *J. Cereb. Blood Flow Metab*. 30:1487–93
14. Mak SK, *et al*. (2012) Small molecules greatly improve conversion of human-induced pluripotent stem cells to the neuronal lineage. *Stem Cells Int*. 2012:140427.
15. Parsons XH. (2012) MicroRNA profiling reveals distinct mechanisms governing cardiac and neural lineage-specification of pluripotent human embryonic stem cells. *J. Stem Cell Res. Ther*. 2.
16. Mohyeldin A, Garzon-Muvdi T, Quinones-Hinojosa A. (2010) Oxygen in stem cell biology: a critical component of the stem cell niche. *Cell Stem Cell*. 7:150–61.
17. Yoshida Y, Takahashi K, Okita K, Ichisaka T,

Yamanaka S. (2009) Hypoxia enhances the generation of induced pluripotent stem cells. *Cell Stem Cell*. 5:237–41.
18. Bae D, *et al*. (2012) Hypoxia enhances the generation of retinal progenitor cells from human induced pluripotent and embryonic stem cells. *Stem Cells Dev*. 21:1344–55.
19. Jelkmann W. (2004) Molecular biology of erythropoietin. *Intern. Med*. 43:649–59.
20. Bernaudin M, *et al*. (2000) Neurons and astrocytes express EPO mRNA: oxygen-sensing mechanisms that involve the redox-state of the brain. *Glia*. 30:271–8.
21. Byts N, *et al*. (2008) Essential role for Stat5 in the neurotrophic but not in the neuroprotective effect of erythropoietin. *Cell Death Differ*. 15:783–92.
22. Digicaylioglu M, Lipton SA. (2001) Erythropoietin-mediated neuroprotection involves cross-talk between Jak2 and NF-kappaB signalling cascades. *Nature*. 412:641–7.
23. Sirén AL, *et al*. (2001) Erythropoietin prevents neuronal apoptosis after cerebral ischemia and metabolic stress. *Proc. Natl. Acad. Sci. U. S. A*. 98:4044–9.
24. Brines M, Cerami A. (2005) Emerging biological roles for erythropoietin in the nervous system. *Nat. Rev. Neurosci*. 6:484–94.
25. Sirén AL, Fasshauer T, Bartels C, Ehrenreich H. (2009) Therapeutic potential of erythropoietin and its structural or functional variants in the nervous system. *Neurotherapeutics*. 6:108–27.
26. Cervellini I, *et al*. (2013) Erythropoietin (EPO) increases myelin gene expression in CG4 oligodendrocyte cells through the classical EPO receptor. *Mol. Med*. 19:223–9.
27. Sargin D, Hassouna I, Sperling S, Sirén AL, Ehrenreich H. (2009) Uncoupling of neurodegeneration and gliosis in a murine model of juvenile cortical lesion. *Glia*. 57:693–702.
28. Zhang G, *et al*. (2011) Erythropoietin enhances nerve repair in anti-ganglioside antibody-mediated models of immune neuropathy. *PLoS One*. 6:e27067.
29. Savino C, *et al*. (2006) Delayed administration of erythropoietin and its non-erythropoietic derivatives ameliorates chronic murine autoimmune encephalomyelitis. *J. Neuroimmunol*. 172:27–37.
30. Tsai PT, *et al*. (2006) A critical role of erythropoietin receptor in neurogenesis and post-stroke recovery. *J. Neurosci*. 26:1269–74.
31. Wang L, Zhang Z, Wang Y, Zhang R, Chopp M. (2004) Treatment of stroke with erythropoietin enhances neurogenesis and angiogenesis and improves neurological function in rats. *Stroke*. 35:1732–7.
32. Zhang Y, *et al*. (2012) Impact of inhibition of erythropoietin treatment-mediated neurogenesis in the dentate gyrus of the hippocampus on restoration of spatial learning after traumatic brain injury. *Exp. Neurol*. 235:336–44.
33. Gonzalez FF, *et al*. (2013) Erythropoietin increases neurogenesis and oligodendrogliosis of subventricular zone precursor cells after neonatal stroke. *Stroke*. 44:753–8.
34. Chen ZY, Asavaritikrai P, Prchal JT, Noguchi CT. (2007) Endogenous erythropoietin signaling is required for normal neural progenitor cell proliferation. *J. Biol. Chem*. 282:25875–83.
35. Shingo T, Sorokan ST, Shimazaki T, Weiss S. (2001) Erythropoietin regulates the in vitro and in vivo production of neuronal progenitors by mammalian forebrain neural stem cells. *J. Neurosci*. 21:9733–43.
36. Eckardt S, *et al*. (2007) Hematopoietic reconstitution with androgenetic and gynogenetic stem cells. *Genes. Dev*. 21:409–19.
37. Ying QL, Stavridis M, Griffiths D, Li M, Smith A. (2003) Conversion of embryonic stem cells into neuroectodermal precursors in adherent monoculture. *Nat. Biotechnol*. 21:183–6.
38. Schneider CA, Rasband WS, Eliceiri KW. (2012) NIH Image to ImageJ: 25 years of image analysis. *Nat. Methods*. 9:671–5.
39. Team RDC. (2009) *R: A language and environment for statistical computing*. Vienna, Austria: R Foundation for Statistical Computing. 409 pp.
40. Gray PA. (2008) Transcription factors and the genetic organization of brain stem respiratory neurons. *J. Appl. Physiol*. 104:1513–21.
41. Lopez-Bendito G, Molnar Z. (2003) Thalamocortical development: how are we going to get there? *Nat. Rev. Neurosci*. 4:276–89.
42. Wang Y, *et al*. (2010) Dlx5 and Dlx6 regulate the development of parvalbumin-expressing cortical interneurons. *J. Neurosci*. 30:5334–45.
43. Boulting GL, *et al*. (2011) A functionally characterized test set of human induced pluripotent stem cells. *Nat. Biotechnol*. 29:279–86.
44. Kawasaki H, *et al*. (2000) Induction of midbrain dopaminergic neurons from ES cells by stromal cell-derived inducing activity. *Neuron*. 28:31–40.
45. Liu H, Zhang SC. (2011) Specification of neuronal and glial subtypes from human pluripotent stem cells. *Cell. Mol. Life Sci*. 68:3995–4008.
46. Peljto M, Wichterle H. (2011) Programming embryonic stem cells to neuronal subtypes. *Curr. Opin. Neurobiol*. 21:43–51.
47. Conti L, *et al*. (2005) Niche-independent symmetrical self-renewal of a mammalian tissue stem cell. *PLoS Biol* 3:e283.
48. Song HJ, Stevens CF, Gage FH. (2002) Neural stem cells from adult hippocampus develop essential properties of functional CNS neurons. *Nat. Neurosci*. 5:438–45.
49. Koehler KR, *et al*. (2012) Extended passaging increases the efficiency of neural differentiation from induced pluripotent stem cells. *BMC Neurosci*. 12:82.
50. Wernig M, *et al*. (2007) In vitro reprogramming of fibroblasts into a pluripotent ES-cell-like state. *Nature*. 448:318–24.
51. Tsuji O, *et al*. (2010) Therapeutic potential of appropriately evaluated safe-induced pluripotent stem cells for spinal cord injury. *Proc. Natl. Acad. Sci. U. S. A*. 107:12704–9.
52. Bock C, *et al*. (2011) Reference maps of human ES and iPS cell variation enable high-throughput characterization of pluripotent cell lines. *Cell*. 144:439–52.
53. Kaichi S, *et al*. (2010) Cell line-dependent differentiation of induced pluripotent stem cells into cardiomyocytes in mice. *Cardiovasc. Res*. 88:314–23.
54. Kuhn HG, Winkler J, Kempermann G, Thal LJ, Gage FH. (1997) Epidermal growth factor and fibroblast growth factor-2 have different effects on neural progenitors in the adult rat brain. *J. Neurosci*. 17:5820–9.
55. Qian X, Davis AA, Goderie SK, Temple S. (1997) FGF2 concentration regulates the generation of neurons and glia from multipotent cortical stem cells. *Neuron*. 18:81–93.
56. Wang L, *et al*. (2007) The Sonic hedgehog pathway mediates carbamylated erythropoietin-enhanced proliferation and differentiation of adult neural progenitor cells. *J. Biol. Chem*. 282:32462–70.
57. Wang L, *et al*. (2006) Neurogenin 1 mediates erythropoietin enhanced differentiation of adult neural progenitor cells. *J. Cereb. Blood Flow Metab*. 26:556–64.
58. Wang Y, *et al*. (2010) Erythropoietin promotes spinal cord-derived neural progenitor cell proliferation by regulating cell cycle. *Neuroscience*. 167:750–7.
59. Torroglosa A, *et al*. (2007) Nitric oxide decreases subventricular zone stem cell proliferation by inhibition of epidermal growth factor receptor and phosphoinositide-3-kinase/Akt pathway. *Stem Cells*. 25:88–97.
60. Kilic E, *et al*. (2005) Brain-derived erythropoietin protects from focal cerebral ischemia by dual activation of ERK-1/-2 and Akt pathways. *Faseb. J*. 19:2026–8.
61. Oh DH, Lee IY, Choi M, Kim SH, Son H. (2012) Comparison of neurite outgrowth induced by erythropoietin (EPO) and carbamylated erythropoietin (CEPO) in hippocampal neural progenitor cells. *Korean J. Physiol. Pharmacol*. 16:281–5.